

1 *Supplement of*

2 **A one-year ACSM source analysis of organic aerosol particle**
3 **contributions from anthropogenic sources after long-range transport**
4 **at the TROPOS research station Melpitz**

5 Samira Atabakhsh et al.

6 *Correspondence to:* Hartmut Herrmann (herrmann@tropos.de)

7 **1 Source apportionment of organic aerosol**

8 This work conducted the most advanced source apportionment analysis following a standardized protocol developed by Chen
9 et al., (2022). In this study, to better identify the organic aerosol (OA) sources in Melpitz, positive matrix factorisation (PMF)
10 was applied on each separate season, following a standardized protocol developed by Chen et al., (2022). Since the
11 measurements were taken between September 2016 and August 2017 (12 months), therefore dataset was split into four
12 meteorological seasons (i.e., fall (September-November); winter (December-February); spring (March-May), and summer
13 (June-August)). Details of the rolling PMF can be found in Chen et al., (2022).

14 **1.1 PMF pre-test**

15 First, to estimate the potential sources in different seasons, unconstrained PMF was applied with different factors (from 4 to
16 6) runs on each season separately. Considering the residential heating during winter time, it was estimated to have the
17 maximum coal combustion OA (CCOA) and biomass burning OA (BBOA) emissions in this season. Therefore, in order to
18 identify and split the sources of solid fuels, the winter season was comprehensively analyzed. However, clear primary factor
19 profiles did not result from unconstrained PMF during the winter season. Therefore, profiles of two primary factors as
20 hydrocarbon-like OA (HOA) and BBOA were constrained by various *a-values* and applying the reference profiles by Crippa
21 et. Al. (2013) and Ng et al. (2011a) for HOA and BBOA, respectively as suggested by Chen et al. (2021). After HOA and
22 BBOA constraining, a third primary factor could be dedicated as well. This new primary factor presented signals which are
23 common in CCOA profiles (e.g., signals from unsaturated hydrocarbons and polycyclic aromatic hydrocarbons (PAHs)). The
24 bootstrap resampling strategy was applied to the input data matrix to check the reliability of the discovered CCOA factor
25 (Davison and Hinkley, 1997). Three primary factors (HOA, BBOA, and resulted CCOA) were used to constrain the PMF
26 solution. Finally, based on residual analysis, it was possible to determine the number of oxygenated OA (OOA). When the

27 number of factors was increased to 6 or more, either the OOAs or the CCOA were split. As a result, throughout the
28 measurements, the five-factor solution with three primary factors and two OOA factors was preferred.
29 PMF with the rolling window approach was performed based on these seasonal pre-tests. The following section describes the
30 specific settings used in this study. Since this approach resulted in an immense number of single PMF solutions, it was
31 necessary to identify and distinguish environmentally reasonable PMF solutions, by using properly selected user-defined
32 criteria. The unconstrained factors were also identified and sorted using these criteria. The particular details of the factors are
33 discussed further below.
34 The correlation of NO_x with HOA factor is used as a HOA criterion since it is known as a typical tracer for traffic emissions.
35 However, to determine if the difference in this correlation was considerable in comparison with the correlation of NO_x with
36 other factors, a *t-test* was performed that solutions with a *p-value* ≤ 0.05 were considered acceptable for all the criteria. For the
37 BBOA factor, the explained variation of m/z 60 was selected as a criterion, since BBOA is typically composed of anhydrous
38 sugar fragments (e.g., levoglucosan fragments m/z 60 and 73). Moreover, the correlation of levoglucosan with BBOA was
39 used as the second criterion for this factor. For the CCOA factor, unsaturated hydrocarbon and polycyclic aromatic
40 hydrocarbon (PAH) signals at m/z 41, 51, 53, 55, 69, 77, 91, and 115 characterize coal combustion emissions (Dall'Osto et al.,
41 2013; Elser et al., 2016; Lin et al., 2017; Xu et al., 2020). Therefore, as a CCOA criterion, the explained variation of m/z 115
42 was selected. Further, the R^2 value of the time series of POA factors (HOA, BBOA, and CCOA) vs equivalent black carbon
43 (eBC) was used for them as other criteria. The unconstrained OOA factors were split by less oxidized oxygenated OA (LO-
44 OOA) and more oxidized oxygenated OA (MO-OOA). We used f_{44} for the MO-OOA as suggested by (Chen et al., 2021)
45 which LO-OOA simply followed by f_{43} .

46 **1.2 Rolling PMF**

47 Following the analysis of the seasonal PMF solutions (i.e., pre-test PMF), rolling PMF was carried out. The shift parameter
48 (the number of days), the width of the window (the number of consecutive days), and the number of repetitions for each PMF
49 window define the rolling PMF approach (Canonaco et al., 2021). Here, to detect source variation, the PMF window with a
50 length of 14 days with a 1-day shift was applied as suggested by (Chen et al., 2021). To compare the four different PMF
51 analyses, the same criteria and thresholds have been used.

52 To investigate the statistical uncertainties of the rolling PMF, repeats per window are needed. However, statistical uncertainty
53 could be evaluated by using the bootstrap strategy, which resamples the PMF input at random. When the factors are constrained
54 by prior knowledge (i.e., reference profiles or external time series), a sensitivity analysis of the *a-value* must be done to
55 investigate the rotational ambiguity. The *a-values* in this study were selected at random for each PMF repetition, ranging from
56 0 to 0.4 for HOA and BBOA, and 0.5 for CCOA ($\Delta a = 0.1$ for all). Based on the criteria described above, 15165 solutions
57 (42.36 %) of the overall 35800 single PMF runs were produced in the rolling PMF approach. All measured time points were
58 modeled within the context of a rolling PMF. As presented in Fig. S1, no systematic errors were observed during the evaluation
59 of the scaled residual over time and variables (m/z).

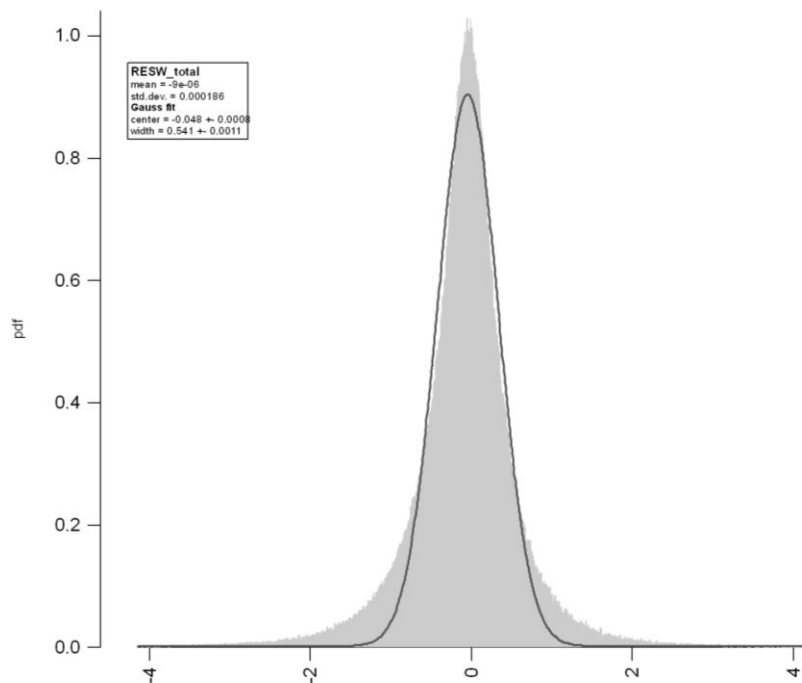


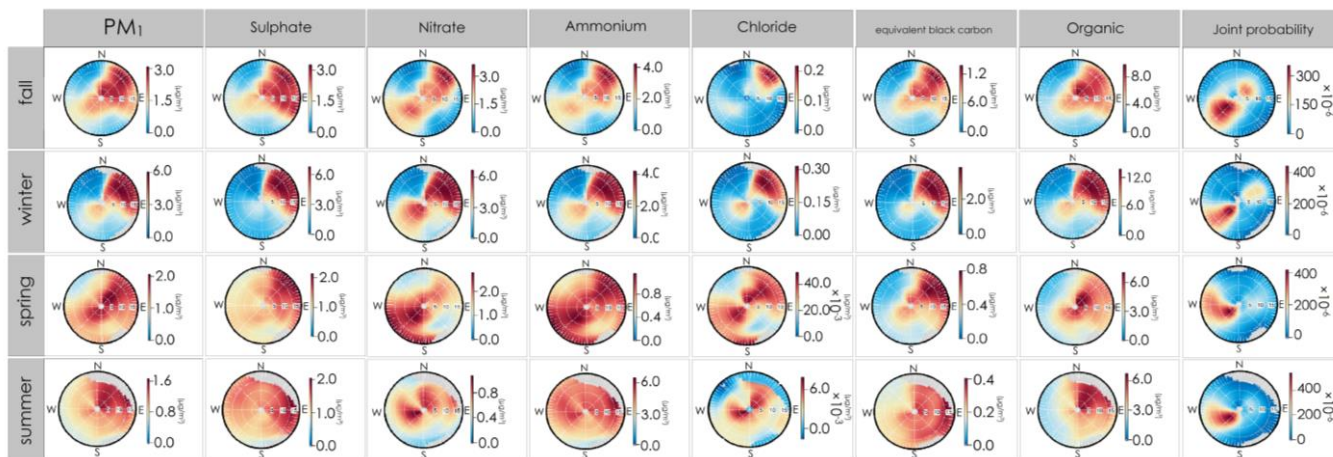
Fig. S1: Analysis of the scaled residuals for the total scaled residuals.

61

62

63

64



65

66 Fig. S2: Seasonal wind roses and NWR plots for the different chemical compositions (in $\mu\text{g}/\text{m}^3$). PM₁ is the average of all the
67 compositions.
68

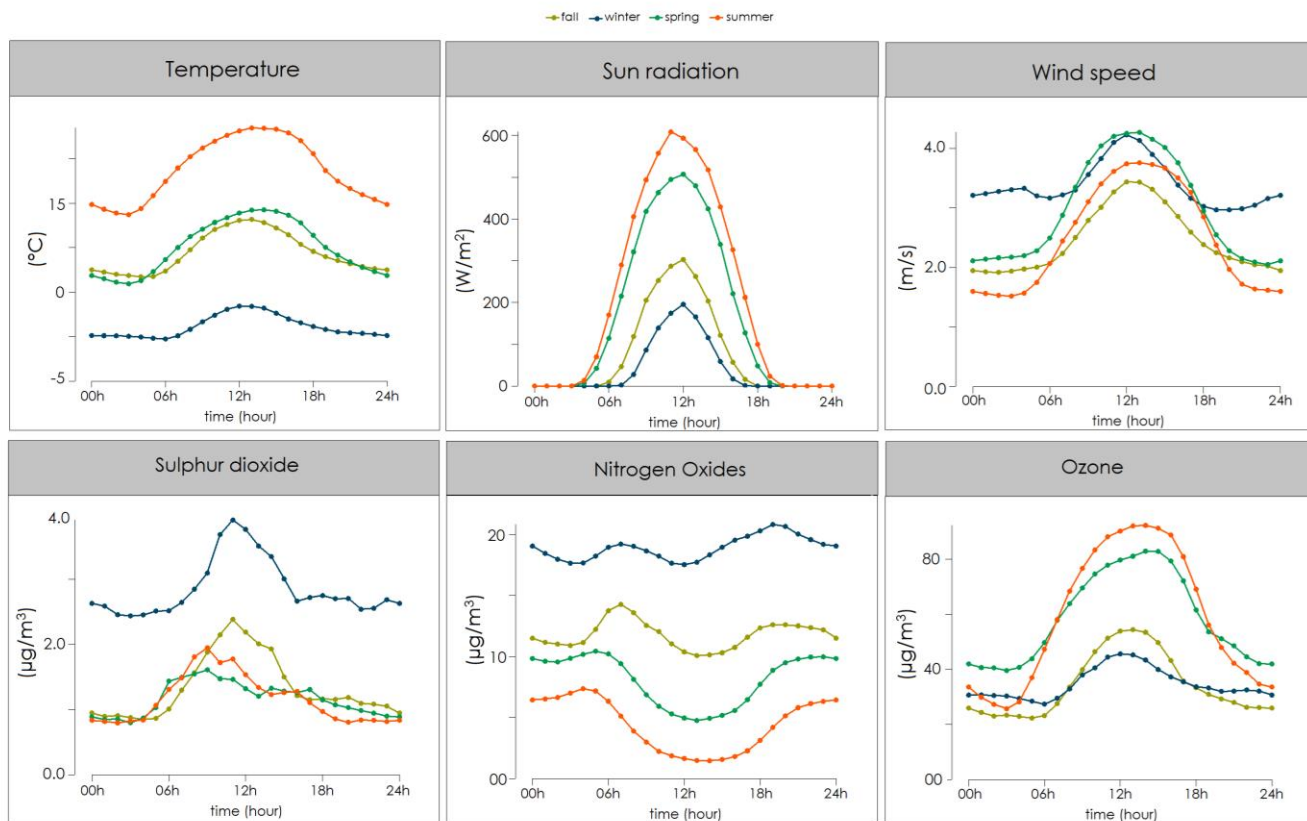


Fig. S3: Seasonal diurnal cycle of Temperature, sun radiation, Sulphur dioxide, Nitrogen Oxides, and Ozone.

Table. S1: PM₁ seasonal mass fraction (%) of each ACSM species, and AMS study (Poulain et al, 2011).

Species	Fall		Winter		Summer	
	ACSM	AMS	ACSM	AMS	ACSM	AMS
Org	55	32	46	23	63	59
SO ₄ ²⁻	16	17	12	18	16	22
ACSM NO ₃ ⁻	16	23	25	34	10	5
NH ₄ ⁺	7	12	10	17	7	8
Cl ⁻	0	0	1	2	0	0
MAAP eBC	6	10	6	6	4	6

69
70
71
72
73

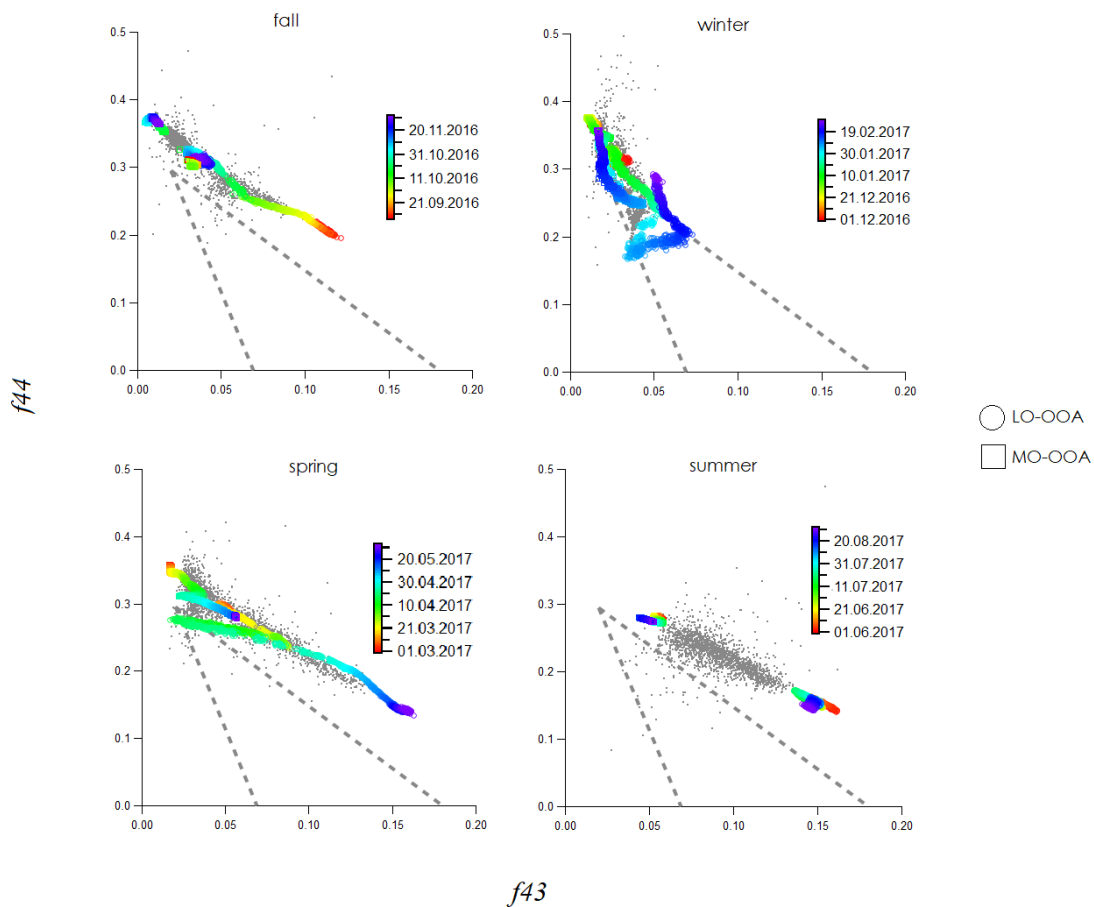
74
75
76
77
78
79
80

81
82
83

Table. S2: Studies information, Current study, Crippa et al., 2014, van Pinxteren et al., 2016 and 2023.

Information	Current study	Crippa et al., 2014	van Pinxteren et al., 2016	van Pinxteren et al., 2023
Instrument	ACSM	AMS	Berner-type cascade impactor	Digitel DHA-80 high-volume filter samplers
PM size	1 μm	1 μm	0.05, 0.14, 0.42, 1.2, 3.5, and 10 μm	10 μm
PM type	Organic	Organic	Total mass	Total mass
Data coverage	1 year (Sep 2016-Aug2017)	2 spring, 1 fall	21 days per: 1 summer, 1 winter	1 year (Nov2018- Oct2019)
Sources category	HOA, BBOA, CCOA, LO-OOA, MO-OOA	HOA, BBOA, LO-OOA, MO-OOA	Crustal material, Salt, Secondary I, II, Biomass combustion, Coal combustion	Traffic, Tr. Exhaust, CCOA, BBOA, SA, Photochem, Cooking, Spores, Urban dust, Sea salt

84
85



86

f_{43}

87

88 **Fig. S4: f_{44} vs. f_{43} for OOA factors (after subtraction of signals contributed by the primary HOA, BBOA, and CCOA factors as**
 89 **shown in Eq. (S1) and (S2)) in hourly resolution, colour coded by date. The triangle plot established by Ng et al., (2010), depicts the**
 90 **region where several PMF OOA from the last decade resided in the f_{44} vs f_{43} space**
 91

92

$$\text{subtracted } f_{44} = \frac{\text{mass conc. of OOA @ } [m/z_{44}]}{\text{mass conc. of OOA + residual of total OA}} \quad (\text{S1})$$

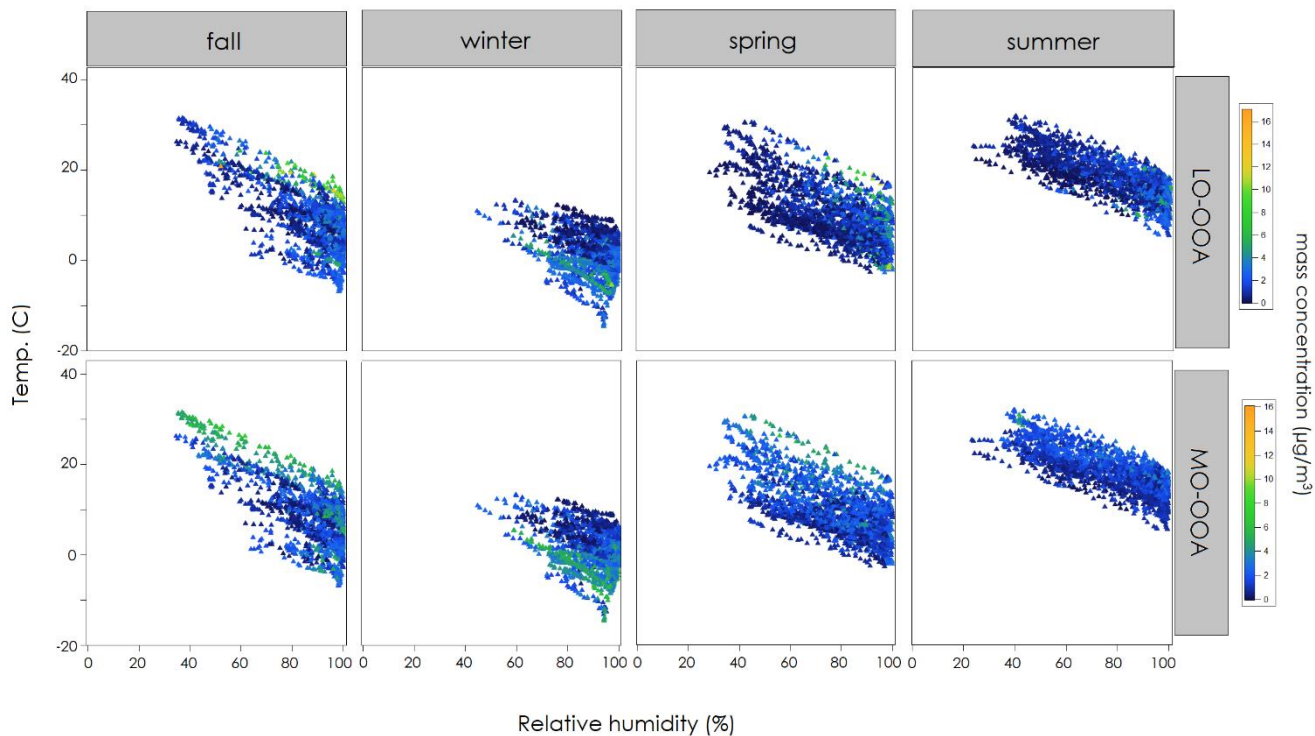
93

94

$$\text{subtracted } f_{43} = \frac{\text{mass conc. of OOA @ } [m/z_{43}]}{\text{mass conc. of OOA + residual of total OA}} \quad (\text{S2})$$

95

96



97
98 **Fig. S5: Temperature (T) and relative humidity (RH) dependence variations of the mass loadings of two OOA fractions.**
99

100
101
102
103 **Table. S3: Linear regression coefficient for m_{HOA} , m_{BBOA} , and m_{CCOA} , defined as a, b, and c for HOA, BBOA, and CCOA;**
104 **respectively.**
105

Factor	Fall	Winter	Spring	Summer
a (HOA)	0.38	0.55	0.11	0.17
b (BBOA)	0.95	0.52	0.65	0.75
c (CCOA)	0.32	0.46	0.35	0.09

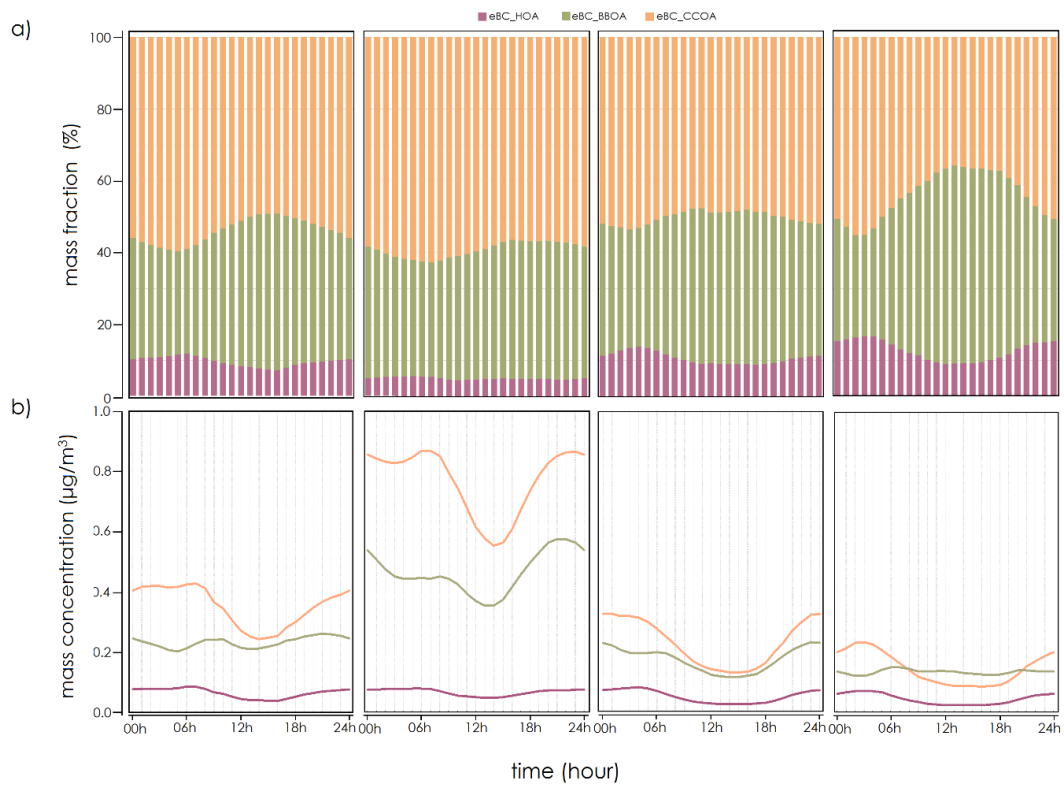
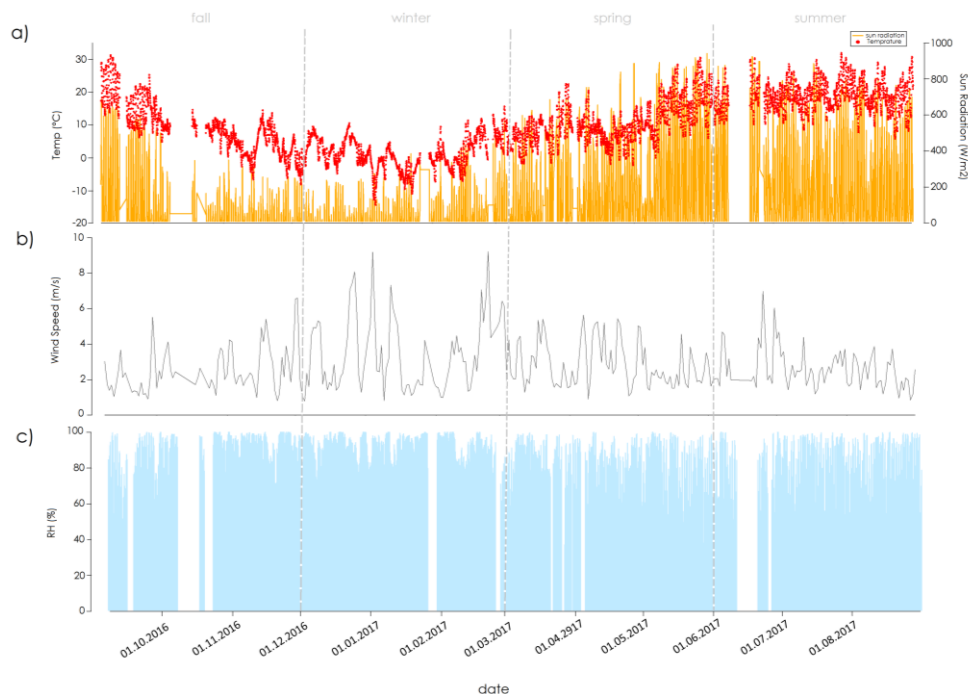


Fig. S6: The diurnal variation of different eBC, a) mass fraction, b) mass concentration of the POA for different seasons.

115
116
117
118
119



120

121 **Fig. S7: Time series of meteorological variables; a) hourly resolution of Temperature in red dots, Sun radiation in yellow line, b)**
 122 **daily resolution of Wind speed and c) hourly resolution of Relative Humidity**

123

124 **Table. S4: Main statistical details of the fifteen air mass types for PM₁ and PMF factors (CS=Cold Season, WS=Warm Season,**
 125 **ST=Stagnant, A=Anticyclonic, C=Cyclonic) based on mass concentration (µg/m³).**

126

Main season	Airmass type	Wind direction	Vorticity	Average mass concentration (µg/m ³)											
				eBC-HOA	eBC-BBOA	eBC-CCOA	NO _x	SO ₂	NH ₄ ⁺	Cl ⁻	HOA	BBOA	CCOA	LO_OOA	MO_OOA
Winter	CS-ST	Stagnating	Anticyclonic	0.06	0.62	0.91	5.38	3.33	2.78	0.14	0.35	0.97	1.89	2.73	2.73
	CS-A1	East	Anticyclonic	0.08	0.67	1.93	5.60	5.39	3.44	0.24	0.49	1.06	4.01	2.72	3.45
	CS-A2	West	Anticyclonic	0.04	0.24	0.31	3.86	1.83	1.89	0.13	0.25	0.38	0.65	1.77	1.97
	CS-C1	South	Cyclonic	0.05	0.38	0.40	2.62	2.99	1.75	0.06	0.30	0.61	0.84	2.17	3.77
	CS-C2a	South West	Cyclonic	0.01	0.07	0.06	1.16	0.78	0.58	0.03	0.07	0.11	0.13	0.30	0.72
CS-C2b	West	Cyclonic	0.01	0.04	0.05	0.35	0.74	0.26	0.02	0.07	0.07	0.10	0.29	0.55	
Transition (Spring/ Fall)	TS-A1	North East	Anticyclonic	0.03	0.11	0.13	1.08	1.07	0.59	0.04	0.17	0.17	0.27	1.03	1.31
	TS-A2	West	Anticyclonic	0.02	0.09	0.08	1.54	1.05	0.73	0.03	0.11	0.15	0.18	0.60	1.23
	TS-C1	South West	Cyclonic	0.02	0.12	0.15	0.77	0.68	0.36	0.01	0.15	0.19	0.31	0.65	1.24
	TS-C2	North West	Cyclonic	0.01	0.07	0.08	1.35	0.90	0.68	0.06	0.09	0.12	0.18	0.50	0.84
Summer	WS-ST	Stagnating	Anticyclonic	0.04	0.21	0.17	1.01	1.88	0.71	0.01	0.23	0.34	0.36	1.10	2.84
	WS-A1	South East	Anticyclonic	0.06	0.32	0.62	3.20	3.25	1.96	0.10	0.34	0.51	1.28	2.15	3.11
	WS-A2	North West	Anticyclonic	0.03	0.14	0.21	2.22	1.63	1.09	0.04	0.19	0.23	0.44	1.13	2.09
	WS-C1	West	Cyclonic	0.03	0.16	0.15	1.63	1.86	0.90	0.03	0.17	0.25	0.32	0.88	2.00
	WS-C2	West	Cyclonic	0.01	0.08	0.07	0.83	1.20	0.51	0.02	0.09	0.13	0.14	0.37	0.97

127

128 **Table. S5: Main statistical details of the fifteen air mass types for PM₁ PMF factors (CS=Cold Season, WS=Warm Season,**
 129 **ST=Stagnant, A=Anticyclonic, C=Cyclonic) based on contribution (%).**

130

Main season	Airmass type	Wind direction	Vorticity	Average mass contribution (%)											
				eBC-HOA	eBC-BBOA	eBC-CCOA	NO _x	SO ₂	NH ₄ ⁺	Cl ⁻	HOA	BBOA	CCOA	LO_OOA	MO_OOA
Winter	CS-ST	Stagnating	Anticyclonic	0	3	4	25	15	13	1	2	4	9	12	12
	CS-A1	East	Anticyclonic	0	2	7	19	18	12	1	2	4	14	9	12
	CS-A2	West	Anticyclonic	0	2	2	29	14	14	1	2	3	5	13	15
	CS-C1	South	Cyclonic	0	2	3	16	19	11	0	2	4	5	14	24
	CS-C2a	South West	Cyclonic	0	2	2	28	19	14	1	2	3	3	8	18
	CS-C2b	West	Cyclonic	0	2	2	14	29	10	1	3	3	4	11	21
Transition	TS-A1	North East	Anticyclonic	0	2	2	18	18	10	1	3	3	4	17	22

(Spring/ Fall)	TS-A2	West	Anticyclonic	0	2	1	26	18	13	1	2	3	3	10	21
	TS-C1	South West	Cyclonic	1	3	3	17	14	8	0	3	4	7	14	26
	TS-C2	North West	Cyclonic	0	2	2	27	18	14	1	2	3	4	10	17
Summer	WS-ST	Stagnating	Anticyclonic	1	1	2	11	21	8	0	3	4	4	12	32
	WS-A1	South East	Anticyclonic	0	2	4	19	19	11	1	2	3	8	13	18
	WS-A2	North West	Anticyclonic	0	2	2	23	17	12	1	2	2	5	12	22
	WS-C1	West	Cyclonic	0	0	2	19	22	11	0	2	3	4	11	24
	WS-C2	West	Cyclonic	0	2	2	19	27	11	1	2	3	3	8	22

131

132 **References**

133 Canonaco, F., Tobler, A., Chen, G., Sosedova, Y., Gates Slowik, J., Bozzetti, C., Rudolf Daellenbach, K., el Haddad, I., Crippa,
134 M., Huang, R. J., Furger, M., Baltensperger, U., and Prévôt, A. S. H.: A new method for long-term source apportionment
135 with time-dependent factor profiles and uncertainty assessment using SoFi Pro: Application to 1 year of organic aerosol
136 data, *Atmos. Meas. Tech.*, 14(2), 923–943, <https://doi.org/10.5194/amt-14-923-2021>, 2021.

137 Chen, G., Sosedova, Y., Canonaco, F., Fröhlich, R., Tobler, A., Vlachou, A., Daellenbach, K. R., Bozzetti, C., Hueglin, C.,
138 Graf, P., Baltensperger, U., Slowik, J. G., el Haddad, I., and Prévôt, A. S. H.: Time-dependent source apportionment
139 of submicron organic aerosol for a rural site in an alpine valley using a rolling positive matrix factorisation (PMF)
140 window, *Atmos. Chem. Phys.*, 21(19), 15081–15101, <https://doi.org/10.5194/acp-21-15081-2021>, 2021.

141 Chen, G., Canonaco, F., Tobler, A., Aas, W., Alastuey, A., Allan, J., Atabakhsh, S., Aurela, M., Baltensperger, U.,
142 Bougiatioti, A., de Brito, J. F., Ceburnis, D., Chazeau, B., Chebaicheb, H., Daellenbach, K. R., Ehn, M., el Haddad, I.,
143 Eleftheriadis, K., Favez, O., Flentje, H., Font, A., Fossun, K., Freney, E., Gini, M., Green, D.C., Heikkinen, L.,
144 Herrmann, H., Kalogridis, A., Keernik, H., Lhotka, R., Lin, C., Lunder, C., Maasikmets, M., Manousakas, M.I.,
145 Marchand, N., Marin, C., Marmureanu, L., Mihalopoulos, N., Mocnika, G., Nećkia, J., O’Dowd, C., Ovadnevaite, J.,
146 Petera, T., Petita, J.E., Pikridasa, M., Matthew Platt, S., Pokorna, P., Poulain, L., Priestman, M., Riffault, V., Rinaldia,
147 M., Rozanskia, K., Schwarz, J., Sciarea, J., Simon, L., Skiba, A., Slowik, J.G., Sosedova, Y., Stavroulas, I., Styszkoa,
148 K., Teinmaa, E., Timonen, H., Tremper, A., Vasilescu, J., Via, M., Vodicka, P., Wiedensohler, A., Zografou, O., Cruz
149 Minguillon, M., and Prévôt, A. S. H.: European aerosol phenomenology – 8: Harmonised source apportionment of
150 organic aerosol using 22 Year-long ACSM/AMS datasets, *Environment International*, 166,
151 <https://doi.org/10.1016/j.envint.2022.107325>, 2022.

152 Crippa, M., Canonaco, F., Lanz, V. A., Äijälä, M., Allan, J. D., Carbone, S., Capes, G., Ceburnis, D., Dall’Osto, M., Day,
153 D. A., DeCarlo, P. F., Ehn, M., Eriksson, A., Freney, E., Ruiz, L. H., Hillamo, R., Jimenez, J. L., Junninen, H., Kiendler-
154 Scharr, A., Kortelainen, A.-M., Kulmala, M., Laaksonen, A., Mensah, A.A., Mohr, C., Nemitz, E., O’Dowd, C.,
155 Ovadnevaite, J., Pandis, S. N., Petäjä, T., Poulain, L., Saarikoski, S., Sellegri, K., Swietlicki, E., Tiitta, P., Worsnop, D.
156 R., Baltensperger, U., and Prévôt, A. S. H.: Organic aerosol components derived from 25 AMS data sets across Europe
157 using a consistent ME-2 based source apportionment approach, *Atmos. Chem. Phys.*, 14(12), 6159–6176,
158 <https://doi.org/10.5194/acp-14-6159-2014>, 2014.

159 Crippa, M., Decarlo, P. F., Slowik, J. G., Mohr, C., Heringa, M. F., Chirico, R., Poulain, L., Freutel, F., Sciare, J., Cozic, J.,
160 di Marco, C. F., Elsasser, M., Nicolas, J. B., Marchand, N., Abidi, E., Wiedensohler, A., Drewnick, F., Schneider, J.,

161 Borrmann, S., Nemitz, E., Zimmermann, R., Jaffrezo, J.-L., Prevot, A. S. H., and Baltensperger, U. Wintertime aerosol
162 chemical composition and source apportionment of the organic fraction in the metropolitan area of Paris, *Atmos. Chem.*
163 *Phys.*, 13(2), 961–981, <https://doi.org/10.5194/acp-13-961-2013>, 2013.

164 Dall’Osto, M., Ovadnevaite, J., Ceburnis, D., Martin, D., Healy, R. M., O’Connor, I. P., Kourtchev, I., Sodeau, J. R., Wenger,
165 J. C., and O’Dowd, C.: Characterization of urban aerosol in Cork city (Ireland) using aerosol mass spectrometry, *Atmos.*
166 *Chem. Phys.*, 13(9), 4997–5015, <https://doi.org/10.5194/acp-13-4997-2013>, 2013.

167 Davison, A. C., and Hinkley, D. V.: *Bootstrap methods and their application*, Cambridge University Press, 1997.

168 Elser, M., Huang, R. J., Wolf, R., Slowik, J. G., Wang, Q., Canonaco, F., Li, G., Bozzetti, C., Daellenbach, K. R., Huang, Y.,
169 Zhang, R., Li, Z., Cao, J., Baltensperger, U., El-Haddad, I., and André, P.: New insights into PM_{2.5} chemical
170 composition and sources in two major cities in China during extreme haze events using aerosol mass spectrometry,
171 *Atmos. Chem. Phys.*, 16(5), 3207–3225, <https://doi.org/10.5194/acp-16-3207-2016>, 2016.

172 Lin, C., Ceburnis, D., Hellebust, S., Buckley, P., Wenger, J., Canonaco, F., Prévôt, A. S. H., Huang, R. J., O’Dowd, C., and
173 Ovadnevaite, J.: Characterization of Primary Organic Aerosol from Domestic Wood, Peat, and Coal Burning in Ireland,
174 *Environ. Sci. Technol.*, 51(18), 10624–10632, <https://doi.org/10.1021/acs.est.7b01926>, 2017.

175 Ng, N. L., Canagaratna, M. R., Jimenez, J. L., Zhang, Q., Ulbrich, I. M., and Worsnop, D. R.: Real-time methods for
176 estimating organic component mass concentrations from aerosol mass spectrometer data, *Environ. Sci. Technol.*, 45(3),
177 910–916. <https://doi.org/10.1021/es102951k>, 2011.

178 Ng, N. L., Canagaratna, M. R., Zhang, Q., Jimenez, J. L., Tian, J., Ulbrich, I. M., Kroll, J. H., Docherty, K. S., Chhabra, P.
179 S., Bahreini, R., Murphy, S. M., Seinfeld, J. H., Hildebrandt, L., Donahue, N. M., Decarlo, P. F., Lanz, V. A., Prévôt,
180 A. S. H., Dinar, E., Rudich, Y., and Worsnop, D. R.: Organic aerosol components observed in Northern Hemispheric
181 datasets from Aerosol Mass Spectrometry, *Atmos. Chem. Phys.*, 10(10), 4625–4641, [https://doi.org/10.5194/acp-10-](https://doi.org/10.5194/acp-10-4625-2010)
182 [4625-2010](https://doi.org/10.5194/acp-10-4625-2010), 2010.

183 Poulain, L., Spindler, G., Birmili, W., Plass-Dülmer, C., Wiedensohler, A., and Herrmann, H.: Seasonal and diurnal variations
184 of particulate nitrate and organic matter at the IfT research station Melpitz, *Atmos. Chem. Phys.*, 11(24), 12579–12599.
185 <https://doi.org/10.5194/acp-11-12579-2011>, 2011.

186 van Pinxteren, D., Fomba, K. W., Spindler, G., Müller, K., Poulain, L., Iinuma, Y., Löschau, G., Hausmann, A., and
187 Herrmann, H.: Regional air quality in Leipzig, Germany: Detailed source apportionment of size-resolved aerosol
188 particles and comparison with the year 2000, *Faraday Discussions*, 189, 291–315, <https://doi.org/10.1039/c5fd00228a>,
189 2016.

190 van Pinxteren, D., Engelhardt, V., Mothes, F., Poulain, L., Spindler, G., Cuesta, A., Tuch, T., Müller, T., Wiedensohler, A.,
191 and Herrmann, H.: Residential wood combustion in Germany: A twin-site study of local village contributions to
192 particulate pollutants. In preparation 2023.

193